THE JOURNAL OF BIOLOGICAL CHEMISTRY
Vol. 275, No. 29, Issue of July 21, pp. 22202–22212, 2000

Printed in U.S.A.

The Top of the Inserted-like Domain of the Integrin Lymphocyte Function-associated Antigen-1 β Subunit Contacts the α Subunit β-Propeller Domain near β-Sheet 3*

Received for publication, April 5, 2000
Published, JBC Papers in Press, April 25, 2000, DOI 10.1074/jbc.M002883200

Qun Zang‡, Chafen Lu§, Chichi Huang¶, Junichi Takagi, and Timothy A. Springer‖

From the Center For Blood Research and Department of Pathology, Harvard Medical School, Boston, Massachusetts 02115

We find that monoclonal antibody YTA-1 recognizes an epitope formed by a combination of the integrin α_L and β_2 subunits of LFA-1. Using human/mouse chimeras of the α_L and β_2 subunits, we determined that YTA-1 binds to the predicted inserted (I)-like domain of the β_2 subunit and the predicted β-propeller domain of the α_L subunit. Substitution into mouse LFA-1 of human residues Ser^{302} and Arg^{303} of the β_2 subunit and Pro^{78}, Thr^{79}, Asp^{80}, Ile^{365}, and Asn^{367} of the α_L subunit is sufficient to completely reconstitute YTA-1 reactivity. Antibodies that bind to epitopes that are nearby in models of the I-like and β-propeller domains compete with YTA-1 monoclonal antibody for binding. The predicted β-propeller domain of integrin α subunits contains seven β-sheets arranged like blades of a propeller around a pseudosymmetry axis. The antigenic residues cluster on the bottom of this domain in the 1–2 loop of blade 2, and on the side of the domain in β-strand 4 of blade 3. The I domain is inserted between these blades on the top of the β-propeller domain. The antigenic residues in the β subunit localize to the top of the I-like domain near the putative Mg^{2+} ion binding site. Thus, the I-like domain contacts the bottom or side of the β-propeller domain near β-sheets 2 and 3. YTA-1 preferentially reacts with activated LFA-1 and is a function-blocking antibody, suggesting that conformational movements occur near the interface it defines between the LFA-1 α and β subunits.

Lymphocyte function-associated antigen-1 (LFA-1)[1] is a member of the leukocyte integrin family: LFA-1 ($\alpha_L\beta_2$; CD11a/CD18), Mac-1 ($\alpha_M\beta_2$; CD11b/CD18), p150,95 ($\alpha_X\beta_2$; CD11c/CD18), and $\alpha_D\beta_2$ (1, 2). The leukocyte integrins are heterodimers composed of a common β_2 subunit noncovalently associated with different but structurally homologous α subunits (3). LFA-1 is expressed on the cell surface of all leukocytes. Upon activation, LFA-1 binds to its ligands, ICAM-1, -2, and -3 (4–6), and mediates important immunological functions including leukocyte adherence to endothelium, natural killing, and antigen-dependent T and B cell responses (7, 8).

Structure-function studies of LFA-1 are important to understand the molecular basis for cell adhesion through LFA-1. Three extracellular subregions of LFA-1 are critical in ligand binding. The first is a sequence of seven 60-amino acid repeats located in the N-terminal half of the α_L subunit. These seven repeats are a common structural feature of all integrin α subunits. These repeats have been predicted to fold into a β-propeller domain with seven β-sheets (9). The β-propeller domain is toroidal in shape, with the β-sheets arranged around a pseudosymmetry axis like blades of a propeller. Each β-sheet may be termed a "W" after the topology of the four anti-parallel β-strands. Ligand binding has been localized to loops on the "upper" surface of the propeller, in β-sheets 2, 3, and 4 for the integrin α subunits α_{IIb}, α_4, and α_5 (10–14). In contrast to α_{IIb}, α_4, and α_5, the leukocyte integrins contain an additional domain of about 200 amino acids. It is inserted into a loop at the top of the β-propeller domain between β-sheets 2 and 3, and is designated the inserted (I) domain. I domain structures for α_L and α_M have been determined by crystallography (15, 16). The I domain folds into a doubly twisted α/β structure with a ligand binding site known as a metal ion-dependent adhesion site, or MIDAS, in a crevice on its upper face. The third region important for ligand binding by integrins is in the N-terminal half of the β_2 subunit from residue 100 to 340, which is well conserved among different integrin β subunits. This conserved region has been predicted to fold like an I domain with a ligand-binding MIDAS motif (15, 17–19, 57). These three domains also interact with divalent cations, such as Mg^{2+}, Mn^{2+}, and Ca^{2+}, which are required to regulate integrin-ligand interactions (4, 21–25).

Extensive studies including mutagenesis and mapping epitopes of function- blocking or activating antibodies have demonstrated that the I domain and the β-propeller domain of the α_L subunit and the I-like domain of the β_2 subunit cooperatively contribute to ligand binding for LFA-1 (26–30). Furthermore, although conformational change in I domains is now well documented (31–34), little is known about conformational change in the β-propeller or I-like domains of leukocyte integrins. Moreover, the structural basis for interactions between these domains remains unknown. Previously, there has been no direct evidence for structural association between the α subunit β-propeller domain and the β subunit I-like domain, despite their joint role in regulating ligand binding. mAb have been used to show that folding of epitopes in the I-like domain is dependent on association with the α subunit, and that folding of epitopes in the β-propeller domain is dependent on association with the β subunit (35, 36). This mutual dependence raised

* This work was supported by Grant CA31798 from the National Institutes of Health. The costs of publication of this article were defrayed in part by the payment of page charges. This article must therefore be hereby marked "*advertisement*" in accordance with 18 U.S.C. Section 1734 solely to indicate this fact.

‡ Present address: Biogen, Inc., Cambridge, MA 02142.
§ Present address: Millennium Pharmaceuticals, Cambridge, MA 02142.
¶ Present address: Pfizer Central Research, Groton, CT 06340.
‖ To whom correspondence should be addressed: Center For Blood Research and Dept. of Pathology, Harvard Medical School, 200 Longwood Ave., Boston, MA 02115. Tel.: 617-278-3200; Fax: 617-278-3232.

[1] The abbreviations used are: LFA-1, lymphocyte function-associated antigen-1; mAb, monoclonal antibody; ICAM-1, intercellular adhesion molecule-1; I, inserted; MIDAS, metal ion-dependent adhesion site; FBS, fetal bovine serum.

the possibility of an intimate structural association between the β-propeller and I-like domains. The mAb used in the above studies were demonstrated to be completely dependent for binding on species-specific residues in either the LFA-1 α or β, but not both subunits (35, 36). For example, mAb used to study folding of the β-propeller domain of the human α_L subunit were reactive with $\alpha_L\beta_2$ complexes whether the β_2 subunit was of human, mouse, or chicken origin (36).

Mapping an antibody with an epitope combined from both integrin α and β subunits would elucidate structural information on intersubunit association. We describe here such a mAb, YTA-1. YTA-1 is specific for the human LFA-1 integrin but has properties that distinguish it from other antibodies to LFA-1 (37, 38). It reacts strongly with $CD3^-/CD16^+$ large granular lymphocytes that function as natural killer cells, but not with other peripheral blood lymphocytes that express LFA-1. Furthermore, YTA-1 is mitogenic for natural killer cells and can activate natural killer cytotoxicity. The antibody was established to be specific for LFA-1 based on its ability to bind to transfectants expressing LFA-1 but not the related β_2 integrins Mac-1 or p150,95. In distinction to other described antibodies to LFA-1, binding of YTA-1 to LFA-1 could be competed away by certain mAbs against both the α_L and β_2 subunits (37). In this report, we demonstrate that YTA-1 recognizes an activation-dependent epitope on LFA-1 consisting of residues from both the β_2 subunit and the α_L subunit. We identify these specific amino acid residues and their positions in models of the α_L β-propeller domain and the β_2 I-like domain. Direct association between these subunits is thus demonstrated and localized.

MATERIALS AND METHODS

Cell Lines and Monoclonal Antibodies—293T cells (a human renal epithelial transformed cell line) were grown in Dulbecco's modified Eagle's medium (Life Technologies, Inc.) supplemented with 10% fetal bovine serum (FBS), nonessential amino acids (Life Technologies, Inc.), 2 mM glutamine, and 50 μg/ml gentamicin. Jurkat (human T lymphoma cells) and SKW3 (human T lymphoma cells) were grown in RPMI 1640 medium with 10% FBS and 50 μg/ml gentamicin.

The mouse anti-human α_L mAbs TS1/22, CBR LFA-1/10, CBR LFA-1/1, G25.2, TS2/4, S6F1, TS2/6, May.035, TS2/14, and 25-3-1; the anti-human β_2 mAbs TS1/18, YFC118.3, YFC51, 1C11, GRF-1, CLB LFA-1/1, May.017, L130, CBR LFA-1/7, and CBR LFA-1/2; the anti-human LFA-1 mAb YTA-1; and the rat anti-mouse α_L mAb M17/5.2 have been described previously (35–37, 39, 40).

Human/Mouse Chimeric α_L and β_2 Constructs—Human and mouse α_L and β_2 cDNA were inserted in vector AprM8 (29). As described previously (29), chimeras were named according to the species origin of their segments. For example, h401m442h indicates residues 1–401 are from human, 402–442 are from mouse and 443 to the C terminus are from human. Chimeras and substitution mutants were generated by polymerase chain reaction overlap extension (41). Briefly, 5′ and 3′ primers were designed to include unique restriction sites. Mutations were introduced with a pair of inner complementary primers. After second round polymerase chain reaction, the products were digested and ligated with the corresponding predigested plasmids. All constructs were verified by DNA sequencing.

Transfection—Plasmids for transfection were purified by QIAprep Spin Kit or Maxi Kit (Qiagen, Valencia, CA). 293T cells were transiently transfected with wild type, mutant or chimeric α_L and β_2 constructs (5 μg each) using calcium phosphate precipitates (42, 43). Medium was changed after 7–11 h. Cells were harvested for analysis 48 h after transfection. Jurkat cell lines stably expressing wild type or mutant LFA-1 have been described previously (44).

Flow Cytometry—Cells were washed twice with L15 medium supplemented with 2.5% FBS (L15/FBS). 10^6 cells were incubated with primary antibody (50 μl of 20 μg/ml purified mAb or 1:100 dilution of ascites) on ice for 30 min. Cells were then washed three times with L15/FBS, followed by incubation with 50 μl of a 1:20 dilution of fluorescein isothiocyanate-conjugated goat anti-mouse (anti-rat for primary mAb M17/5.2) IgG (Zymed Laboratories Inc., San Francisco, CA) for 30 min on ice. After washing three times with L15/FBS, cells were resuspended in 200 μl of cold phosphate-buffered saline and analyzed on a FACScan (Becton Dickinson, San Jose, CA). Surface LFA-1 expression

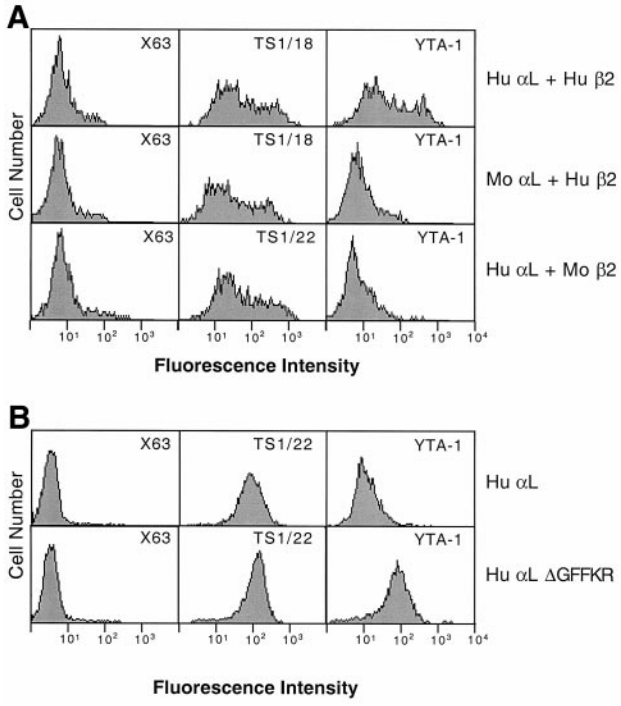

FIG. 1. **mAb YTA-1 is specific for both subunits of human LFA-1.** *A*, 293T cells were co-transfected with cDNA for human or mouse α_L and β_2 subunits, as indicated. *B*, Jurkat-$\beta_{2.7}$ cells were stably transfected with the wild type human α_L subunit or mutated human α_L subunit in which the GFFKR sequence at the junction of the transmembrane and cytoplasmic domains was deleted (44). Transfectants were stained with TS1/18 mAb to β_2, TS1/22 mAb to α_L, YTA-1 mAb, or X63 myeloma IgG1 as control. Cells were then stained with fluorescein isothiocyanate anti-Ig and subjected to immunofluorescence flow cytometry.

is presented as the mean fluorescence intensity of the scatter-gated cell population.

Competition Assay—YTA-1 antibody was biotinylated according to vender's instructions (Zymed Laboratories Inc.). Briefly, the antibody was dialyzed against 0.1 M $NaHCO_3$ buffer (pH 8.3) overnight, incubated with aminohexanoyl-biotin-*N*-hydroxysuccinimide ester for 1 h at room temperature and then dialyzed against phosphate-buffered saline. For competition experiments, cells were preincubated with saturating concentrations of anti-human LFA-1 antibodies on ice for 30 min, washed with phosphate-buffered saline, and further incubated with either control antibody X63 or biotinylated YTA-1 (100 μg/ml) for 30 min. Then, the cells were washed, incubated with 1:100 dilution of phycoerythrin-conjugated streptavidin (Zymed Laboratories Inc.), washed, and analyzed by flow cytometry.

Adhesion Assay—Binding of cells to human soluble ICAM-1 was examined as described (44). Briefly, purified human soluble ICAM-1 was absorbed to each well of flat-bottom 96-well plates by incubation overnight at 4 °C. Nonspecific binding sites were blocked with 1% bovine serum albumin at room temperature for 1 h. Cells were labeled with 2′,7′-bis-(carboxyethyl)-5(and-6)-carboxyfluorescein, acetoxymethyl ester and mixed in ICAM-1-coated wells with 50 μg/ml mAb YTA-1, TS1/22, or as control the X63 myeloma IgGl. After incubation at 37 °C for 15 min, the unbound cells were removed on a Microplate Autowasher (Bio-Tek Instruments, Winooski, VT). The fluorescence content of total input cells (before washing) and the bound cells (after washing) in each well was quantified with a fluorescence concentration analyzer (IDEXX, Westbrook, ME).

α_L Subunit β-Propeller Model—Modeling was with SegMod (45) of LOOK, version 2.0.5 (Molecular Applications Group, Palo Alto, CA) and MODELLER release 4. (46). The β-propeller domain template was the transducin β subunit (Protein Data Bank code 1tbg). A LOOK model was made using the alignment shown below in Fig. 4 between the LFA-1 α_L subunit and the G protein transducin β subunit (47); additionally, three 3–4 loop templates of W5 of 1gof (galactose oxidase) were used as templates for the 3–4 loops of W5, W6, and W7 as described previously (48). The 1–2 loops were then excised from W5–W7 of this model, and Ca^{2+}-binding loops from 1alk (alkaline protease) were superimposed using 4 β-strand residues on either side of this loop from

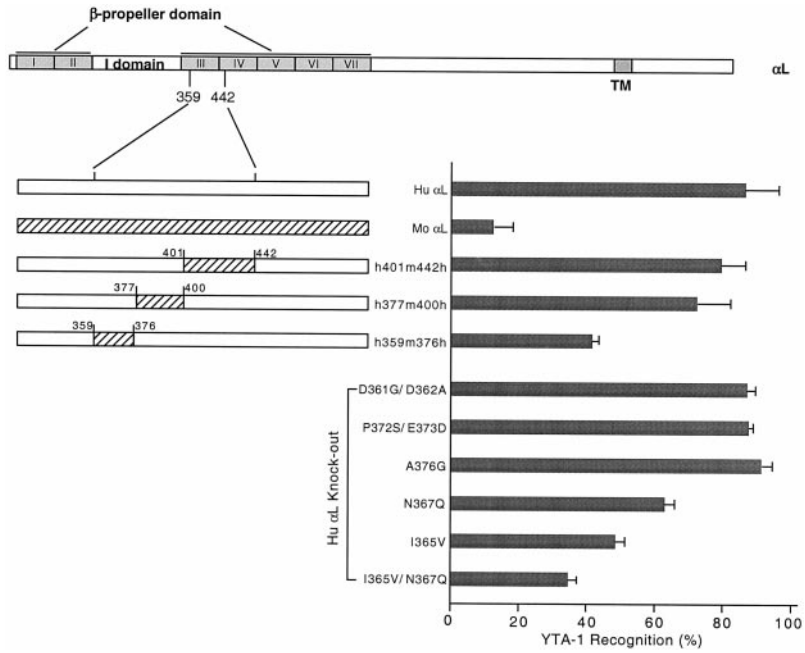

FIG. 2. **Residues Ile[365] and Asn[367] in the human α_L subunit are necessary for YTA-1 recognition.** The indicated human/mouse α_L chimeras and mutants were co-transfected with human β_2 into 293T cells. The transfectants were stained with YTA-1 mAb or TS1/18 mAb to β_2, followed by immunofluorescence flow cytometry. YTA-1 recognition was measured as mean specific fluorescence intensity and quantitated as a percentage of total LFA-1 expression defined by staining with TS1/18 mAb to β_2. Results are the mean ± S.D. of triplicate samples and are representative of three independent experiments.

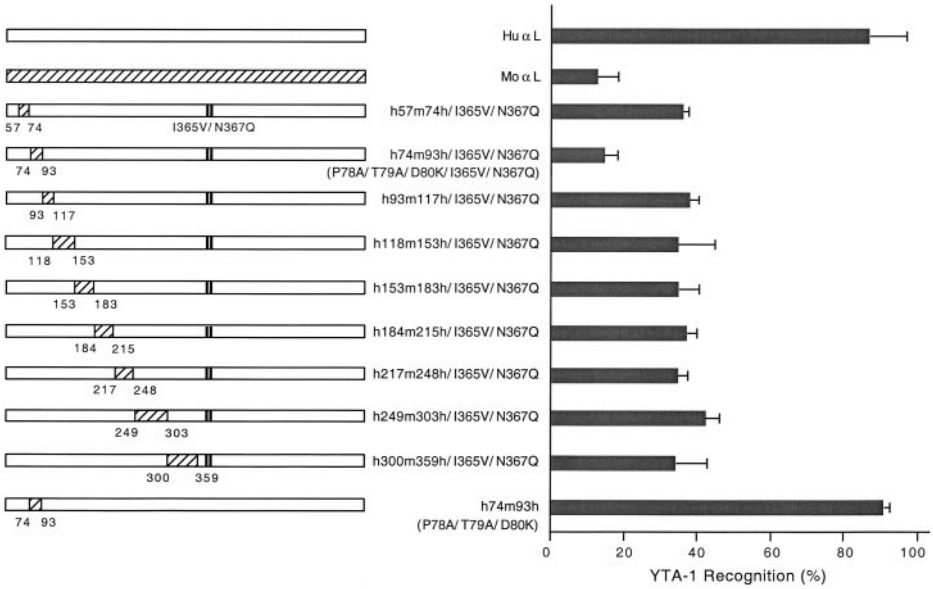

FIG. 3. **Residues Pro[78], Thr[79], and Asp[80] in the human α_L subunit contribute to recognition by YTA-1 mAb.** Human α_L cDNA mutated by introduction of the indicated segments of murine sequence were co-transfected with human β_2 cDNA into 293T cells. YTA-1 recognition was quantified as in Fig. 2.

1alk and 1tbg. A final model was made with MODELLER using the entire LOOK model as the .ini file, and as templates: 1) three different 1alk files containing only the residues shown in Fig. 4 and Ca^{2+} ions, 2) the LOOK model of α_L deleting the residues aligning with the 1alk loops and the residues shown in lowercase in Fig. 4 to enable the two cysteines in this region to form a disulfide using the PATCH DISULFIDE routine, and 3) circularly permuted 1tbg Protein Data Bank files starting with strand 4 of W1 as shown in Fig. 4 and also beginning with strand 4 of W2, W3, and W4 (see Ref. 9). One hundred models were made, and one was chosen that lacked knotted loops, contained Ca^{2+}-binding loops with conformations similar to that of 1alk, and had a score of −1.772 as determined with the QUACHK module of WHAT IF (49).

RESULTS

Monoclonal Antibody YTA-1 Recognizes Human LFA-1 on an Epitope Formed by a Combination of the α_L and β_2 Subunits—To test whether the YTA-1 mouse anti-human antibody was specific for both the human α_L and β_2 subunits, they were expressed in association with murine β_2 and α_L subunits, respectively. Binding of YTA-1 mAb to 293T cell transfectants was measured by immunofluorescence flow cytometry, and the total amount of LFA-1 surface expression was determined with mAb that react with human α_L or β_2 independently of the species origin of the associating subunit (35, 36); expression of LFA-1 on the cell surface requires association between the α_L and β_2 subunits (50, 51). Human LFA-1 and mouse/human hybrid LFA-1 were equivalently expressed, as examined by immunostaining with either TS1/18 mAb to β_2 or TS1/22 mAb to α_L (Fig. 1*A*). MAb YTA-1 was strongly reactive with human LFA-1, but not LFA-1 with human α_L and mouse β_2 or mouse α_L and human β_2 subunits (Fig. 1*A*). Thus, both the α_L and β_2 subunits have to be of human origin to form the YTA-1 epitope. The overall conformation of the mouse/human hybrid LFA-1 molecules was intact as shown by immunostaining with other anti-α_L and β_2 mAbs. Indeed, all other mAbs we have studied, including 11 directed to 7 different epitopes on the α_L subunit, and 17 to 12 different epitopes on the β_2 subunit, are fully reactive if only one of the two subunits is of human origin (35, 36).

We examined whether LFA-1 activation affected the expression of the YTA-1 epitope. Previous studies have shown that LFA-1 expressed in 293T cells is constitutively active in binding ICAM-1 (44) (and see Fig. 9 below). Therefore, we tested

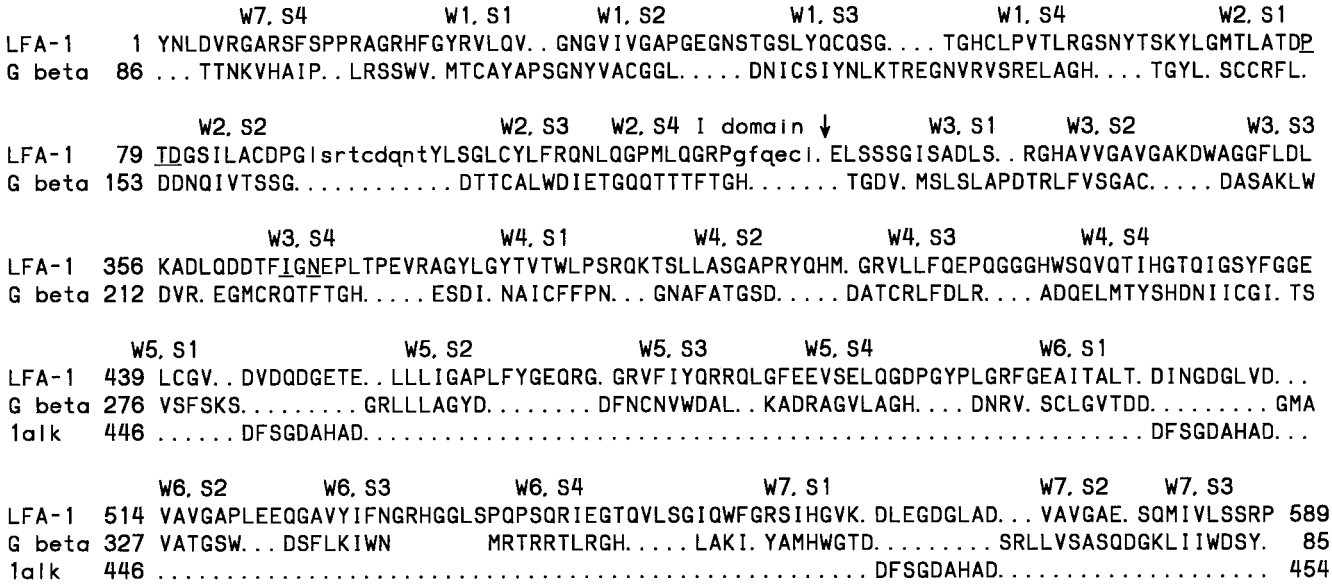

FIG. 4. **Sequence alignment for the LFA-1 α subunit β-propeller domain.** Each β-strand is designated by the β-sheet (*W*) in which it is present and strand position (*S*) in the sheet. Strand 1 is innermost and lines the 7-fold pseudosymmetry axis; strand 4 is outermost and forms the cylindrical side of the β-propeller. N- and C-terminal sequence segments come together to form W7. Antigenic residues recognized by YTA-1 mAb are *underlined*. The LFA-1 β-propeller domain was modeled with this alignment, as described under "Materials and Methods" using the transducin G protein β subunit as the β-propeller template and loops from the bacterial alkaline protease 1akl as templates for Ca^{2+}-binding loops.

LFA-1 in Jurkat T lymphoma cells. A mutant Jurkat cell line (Jurkat-$\beta_{2.7}$) deficient in endogenous α_L subunit was stably transfected with wild type human LFA-1 α_L subunit or an activated form of α_L in which the conserved GFFKR sequence motif in the cytoplasmic domain is deleted (44). The YTA-1 mAb bound much better to activated than wild-type LFA-1 whereas the TS1/22 mAb to LFA-1 bound similarly to activated and wild-type (Fig. 1*B*). The fluorescence intensity of YTA-1 was 74% of that of TS1/22 on activated LFA-1, and only 9% of TS1/22 on wild-type LFA-1. Therefore, YTA-1 preferentially reacts with activated LFA-1.

Mapping the YTA-1 Epitope on the Human α_L Subunit—Mapping was done with mouse-human chimeras named according to the species origin of their segments, *e.g.* h300m359h is an α subunit with human amino acid residues 1–300, mouse residues 301–359, and human residues 360 to C terminus. Previous work showed that "YTA-1 mAb lost reactivity with h300m442h but reacted with h300m359h; thus, at least a portion of its epitope localizes to residues 360–442" (29). To refine this mapping, three different segments of mouse sequence, 359–376, 377–400, and 401–442 were swapped into the human α_L sequence. Chimeric α_L subunits were co-transfected with human β_2 into 293T cells followed by immunostaining with YTA-1 (Fig. 2). Swapping in mouse segments 377–400 or 401–442 had no effect on binding of YTA-1 mAb; however, swapping in 359–376 in chimera h359m376h reduced binding to less than half of that seen with human LFA-1. All chimeras were well expressed and folded, as determined by staining with other mAb to the α_L β-propeller domain and mAb TS1/18 to β_2 (data not shown).

Within region 359–376, seven amino acids differ between human and mouse α_L. Mouse residues were therefore introduced into the human sequence one or two at a time ("knock-out" mutations) (Fig. 2). Three groups of residues had no effect. However, N367Q and I365V each reduced binding. Furthermore, the double mutant I365V/N367Q reduced binding by the same amount as h359m376h.

Although residues Ile^{365} and Asn^{367} appeared to be the only species-specific residues recognized by YTA-1 in the 359–442 segment, YTA-1 reacted more strongly with I365V/N367Q and h359m376h than with mouse α_L (Fig. 2). To determine if residues in other segments were recognized by YTA-1, the I365V/N367Q mutation was introduced into a set of previously constructed α_L chimeras in which small segments within region 1–359 of human α_L were replaced with mouse sequences (29) (Fig. 3). Of all segments tested, only replacement of residues 74–92 with mouse sequence was additive with I365V/N367Q, and reduced binding to the same low level as seen with mouse α_L. However, substitution h74m93h alone was unable to reduce YTA-1 binding (Fig. 3). Comparison of human and mouse α_L sequences within region 74–93 reveals only three differences, at the contiguous amino acid residues 78, 79, and 80. Therefore, substitution of only five residues of the human α_L subunit, Pro^{78}, Thr^{79}, Asp^{80}, Ile^{365}, and Asn^{367}, is sufficient to abolish recognition of the YTA-1 epitope. According to the β-propeller model (9), these residues are located in adjacent β sheets: Pro^{78}, Thr^{79}, and Asp^{80} in β-sheet 2, and Ile^{365} and Asn^{367} in β-sheet 3 (Fig. 4).

To confirm the above "knock-out" results, "knock-in" mutants were made by introducing the corresponding human residues into mouse α_L (Fig. 5). Knock-in mutation V365I/Q367N was sufficient to restore the same level of YTA-1 binding as with human α_L, and the individual V365I and Q367N mutants partially restored binding. The A78P/A79T/K80D knock-in partially reconstituted YTA-1 binding (Fig. 5), consistent with the inability of the I365V/N367Q knock-out to fully eliminate YTA-1 binding (Fig. 3). Combination of the knock-in mutations at residues 78–80 with those at 365 and 367 showed that the knock-in mutations at 365 and 367 were sufficient for YTA-1 binding, and that knocking in residues 78–80 had little additional effect.

Mapping the YTA-1 Epitope on the Human β_2 Subunit—The YTA-1 mAb binding site on the human β_2 subunit was mapped by using human/mouse β_2 chimeras (Fig. 6, *left*). Immunostaining of 293T cells cotransfected with chimeric β_2 and human α_L cDNA showed that region 302–344 is important for YTA-1 recognition. All chimeras in which region 302–344 was of mouse origin failed to stain with YTA-1, whereas all chimeras in which this region was of human origin stained as well as human β_2 (Fig. 6, *right*). Region 302–344 is in the C-terminal portion of the I-like domain (Fig. 6, *upper left*). Controls confirmed that all chimeras stained equally well with mAb that

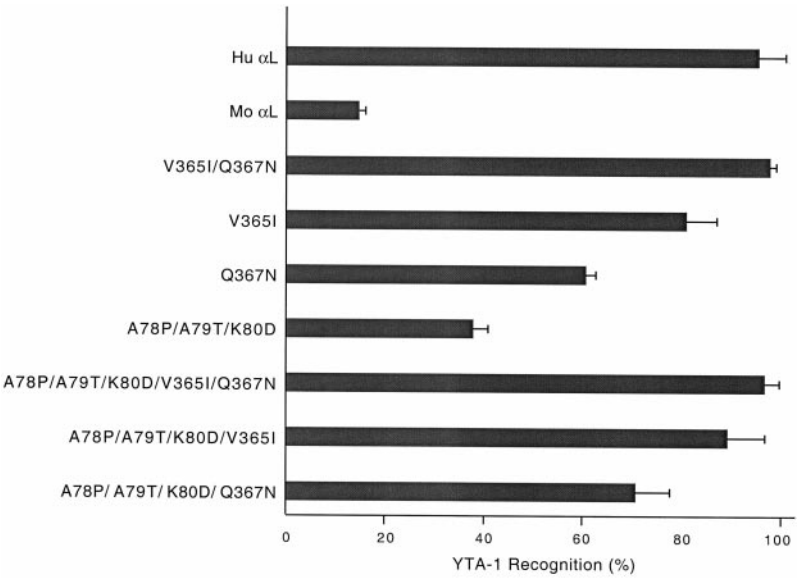

FIG. 5. **Reconstituting YTA-1 mAb binding by knock-in of human residues into the mouse α_L sequence.** The indicated human residues were introduced into the mouse α_L sequence. Each mutant α_L cDNA was co-transfected with human β_2 cDNA into 293T cells. YTA-1 recognition was quantified as in Fig. 2.

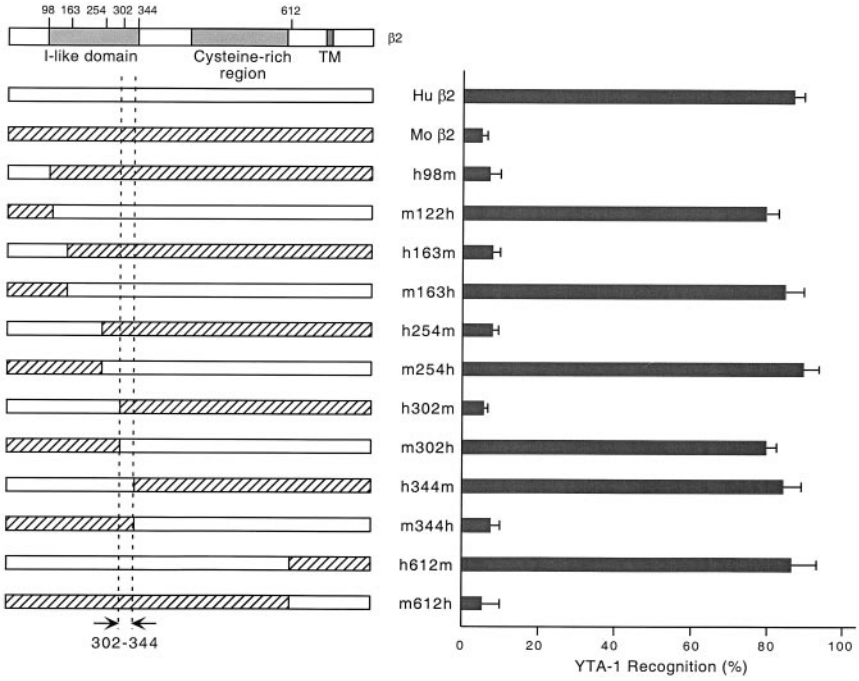

FIG. 6. **YTA-1 recognizes a segment of the I-like domain in the human β_2 subunit.** The indicated human/mouse chimeric β_2 cDNA was co-transfected with human α_L into 293T cells. YTA-1 recognition was quantified by immunofluorescence flow cytometry as described in Fig. 2, except that the amount of YTA-1 recognition was expressed as a percentage of the staining with TS1/22 mAb to human α_L.

map to other epitopes on β_2 and with mAb TS1/22 to α_L.

Only five residues differ between human and mouse β_2 in the segment 302–344: 302, 303, 325, 332, and 339. Specific human residues were "knocked out" by substituting them with mouse residues. The double mutation S302K/R303K completely abolished recognition by YTA-1 (Fig. 7*A*). By contrast, mutation of each of the other three species-specific residues in the 302–344 interval, E325D, H332Q, and N339Y, had no effect on recognition by YTA-1. The TS1/18 mAb was previously reported to block binding of YTA-1 mAb to LFA-1 (37). It has been mapped to residues Arg^{133} and His^{332}, which are predicted to be present on adjacent α-helices in the structure of the β_2 subunit I-like domain (57). Therefore, we also tested the R133Q/H332Q double mutation for recognition by YTA-1, and somewhat surprisingly, found that it abolished recognition by YTA-1. However, the individual substitution R133Q, like H332Q, had no effect on YTA-1 binding. The double mutation R133Q/N339Y also had no effect (Fig. 7*A*).

In reciprocal experiments, human → mouse "knock-in" mutations were introduced into the mouse β_2 subunit. The knock-in mutation K302S/K303R restored YTA-1 reactivity to the same level as seen with the fully human β_2 subunit (Fig. 7*B*). However, the "knock-in" mutation Q133R/Q332H had no effect at all. These results suggest that, in human β_2, residues Ser^{302}/Arg^{303} represent a direct binding site for YTA-1, whereas the involvement of Gln^{133} and His^{332} is indirect.

Reconstitution of the YTA-1 Epitope on Mouse LFA-1—The above experiments indicated that the YTA-1 epitope may contain residues Pro^{78}, Thr^{79}, Asp^{80}, Ile^{365}, and Asn^{367} in the α_L subunit, and Ser^{302} and Arg^{303} in the β_2 subunit of human LFA-1. To test whether these residues are sufficient to form the YTA-1 epitope, mouse α_L and β_2 with these human → mouse "knock-in" mutations were co-transfected into 293 cells and immunostained with YTA-1 (Fig. 8). "Knock-in" of the five human residues into mouse α_L and the two human residues into mouse β_2 reconstituted recognition by YTA-1 to the same level as seen with human LFA-1 (Fig. 8).

Competition of YTA-1 Binding by Other Antibodies to Human

LFA-1—In our previous studies, we mapped a number of anti-LFA-1 antibodies to specific regions or residues in the α_L or β_2 subunits (35, 36, 57). To determine the relationship between these epitopes and the YTA-1 epitope, we tested these antibodies for their ability to compete with YTA-1 for binding to LFA-1. Transfected 293T cells expressing human LFA-1 or Jurkat cells expressing the active, GFFKR deletion mutant of LFA-1 were pre-incubated with an anti-LFA-1 mAb and subsequently immunostained with biotinylated YTA-1 (Table I). All antibodies were independently confirmed to bind to LFA-1 on these two cell types. Ten different mAb to α_L were tested, five of which were directed to epitopes in the β-propeller domain. Among these, only CBR LFA-1/1 blocked binding of YTA-1 to LFA-1 (Table I). This antibody was mapped to region 301–359 (36), nearby residues Ile^{365} and Asn^{367} of the YTA-1 epitope.

Among mAb to β_2, several mAb to the I-like domain blocked YTA-1 binding (Table I). TS1/18, GRF-1, YFC118.3 and YFC5.1 recognize similar but not identical epitopes involving residues Arg^{133} and His^{332}. Human residues must be present at both of these positions for recognition by YFC5.1 and YFC118.3, whereas a human residue at either one of these positions is sufficient for binding by TS1/18 and GRF-1 mAb (57). mAb to both types of epitopes blocked binding of YTA-1 to 293T cell transfectants, whereas only TS1/18 and GRF-1 blocked binding to mutationally activated LFA-1 on Jurkat T lymphoma cells (Table I). This finding was repeatable, and may indicate an indirect relationship between YTA-1 and the Arg^{133}/His^{332} epitopes. Antibodies to other epitopes involving residues 133 and 332 did not block binding: mAb 1C11 specific for Arg^{133} and Asn^{339}, and mAb CLB LFA-1/1 specific for His^{332} and Asn^{339}. Two mAb that recognize Glu^{175} in the I-like domain blocked binding, May.017 and L130 (Table I). All antibodies were independently confirmed to bind to LFA-1 on these two cell types. mAb to two more C-terminal segments in the β subunit, CBR LFA-1/7 and CBR LFA-1/2, did not block binding.

YTA-1 Is a Function-blocking Antibody—We tested whether YTA-1 antibody inhibited LFA-1 binding to its ligand ICAM-1. Human LFA-1 overexpressed on 293T cells was constitutively active in binding to immobilized human ICAM-1 (Fig. 9*A*). However, binding to ICAM-1 was abolished if the cells were

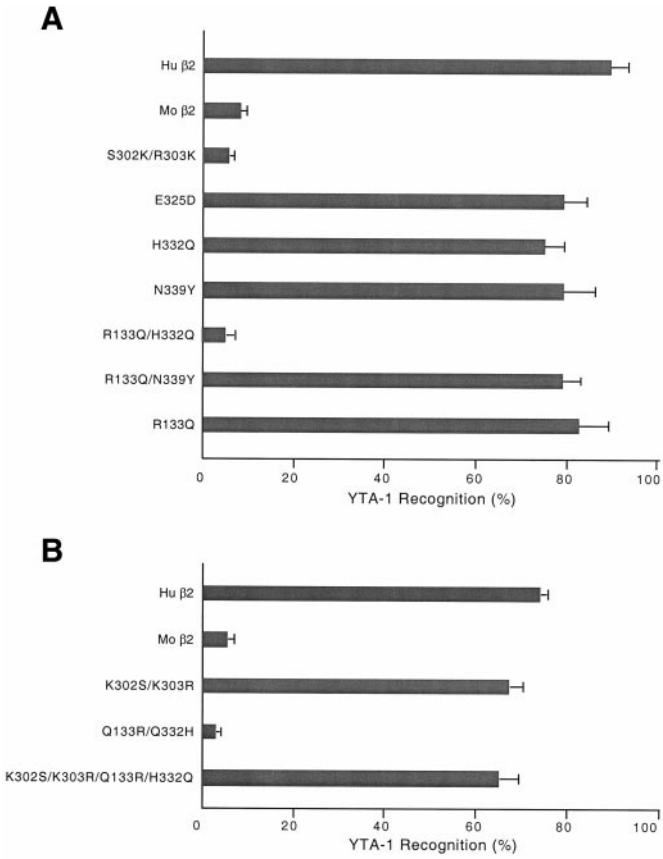

FIG. 7. **Effect of specific amino acid substitutions in the β_2 subunit on the YTA-1 epitope.** *A*, knock-out mutations were made by introducing the indicated mouse residues into the human β_2 sequence. *B*, knock-in mutations were made by introducing the indicated human residues into the mouse β_2 sequence. Each β_2 mutant was co-transfected with human α_L into 293T cells, and YTA-1 recognition was determined by immunofluorescence flow cytometry, as described in Fig. 6.

TABLE I

Competition of YTA-1 binding to human LFA-1 by other antibodies

Human α_L and β_2 were transiently co-transfected into 293 cells. Jurkat cells were stably transfected with activated LFA-1 as described in Fig. 1. The transfectants were preincubated with indicated antibodies and then stained with biotinylated YTA-1 and phycoerythrin-streptavidin. All antibodies bound to the cells, as confirmed in a separate immunofluorescence flow cytometry experiment. The results were reproduced in three independent experiments. −, the antibody did not affect the binding of YTA-1 to LFA-1 (>70% of control); +, the antibody reduced the binding of YTA-1 to LFA-1 to the level of background (<10% of control); +/−, the antibody partially reduced binding of YTA-1 (30–50% of control).

mAb	Epitope	Competition	
		293T cells	Jurkat αΔGFFKR
TS 2/4	β-Propeller of α_L, 1–57(W1)	−	−
S6F1	1–57(W1)	−	−
CBR LFA-1/10	75–117(W2)	−	−
CBR LFA-1/1	301–359(W3)	+	+
G25.2	443–654(W5, 6 and 7)	−	−
TS 2/6	I domain of α_L, 153–183	−	−
May.035	183–215	−	−
TS2/14	248–303	−	−
TS1/22	248–303	−	−
25–3-1	248–303	−	−
TS1/18	I-like domain of β_2, R133 or H332	+	+
GRF-1	R133 or H332	+	+
YFC 118.3	R133 and H332	+	−
YFC 5.1	R133 and H332	+	−
1C11	R133 and N339	−	−
CLB LFA-1/1	H332 and N339	−	−
May.017	E175	+	+
L130	E175	+/−	+
CBR LFA-1/7	Cysteine-rich region of β_2, 345–521	−	−
CBR LFA-1/2	522–612	−	−

FIG. 8. **Reconstitution of the YTA-1 epitope in mouse LFA-1.** 293T cells were co-transfected with human α_L/human β_2, or mouse α_L (A78P/A79T/K80D/V365I/Q367N)/mouse β_2 (K302S/K303R), immunostained with TS1/18 (anti-human β_2), M17/5.2 (anti-mouse α_L), YTA-1, or negative control antibody X63 and analyzed by immunofluorescence flow cytometry. The results were reproduced in three independent experiments.

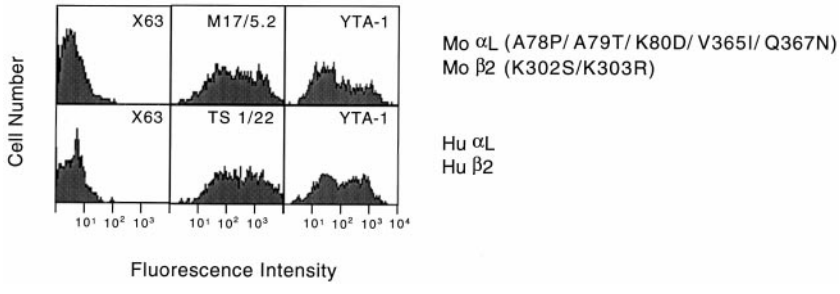

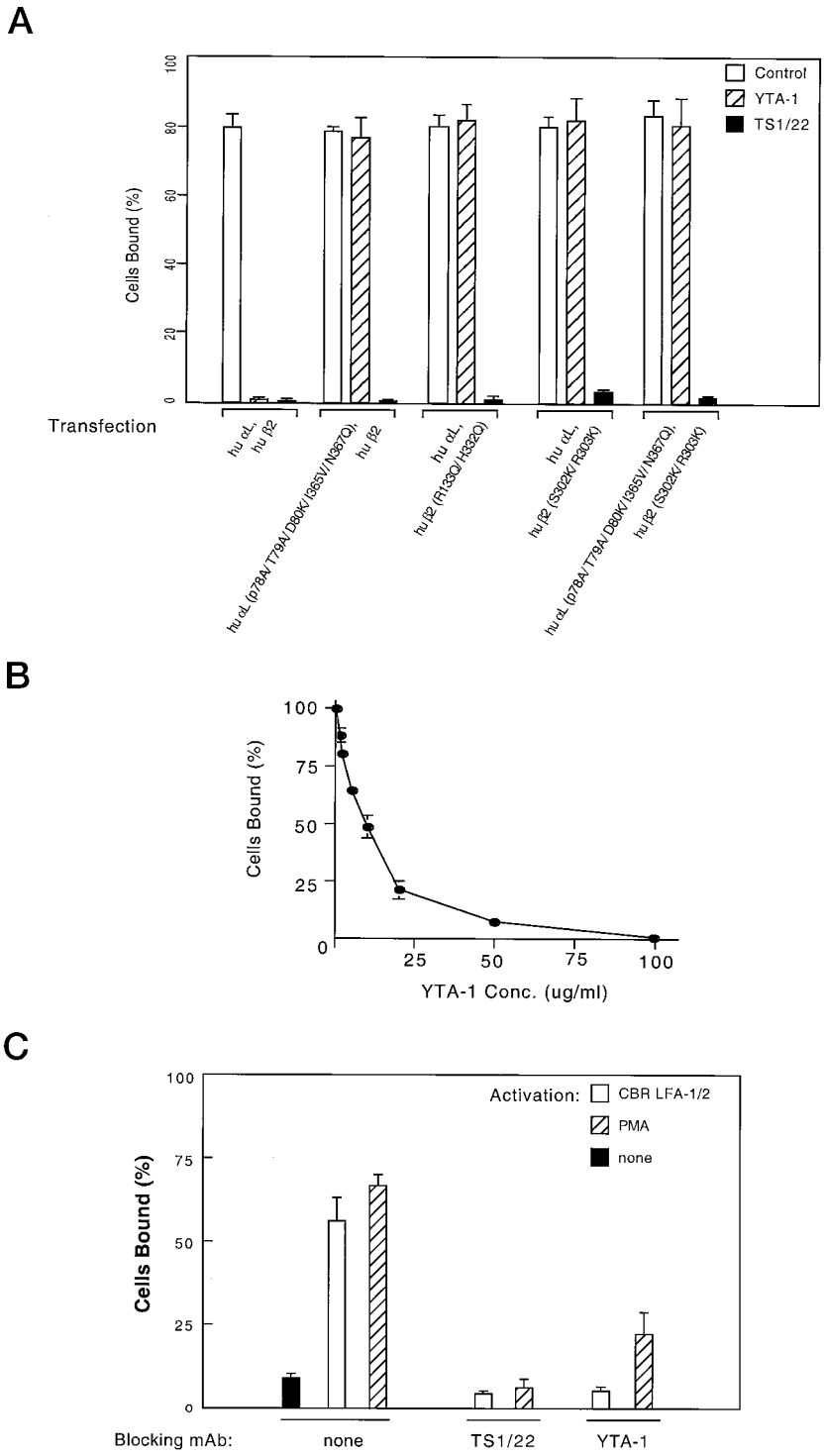

FIG. 9. **YTA-1 inhibits LFA-1 binding to ICAM-1.** Cells were labeled with 2′,7′-bis-(carboxyethyl)-5(and-6)-carboxyfluorescein, acetoxymethyl ester and mixed in ICAM-1-coated wells with or without YTA-1, TS1/22, or control myeloma X63 IgG1. The fluorescence of input cells before washing and the bound cells after washing in each well was quantified on a fluorescent concentration analyzer. Bound cells were calculated as a percentage of total input cells. The results represent at least three independent experiments. *A*, 293T cells were transfected with human LFA-1 or the indicated mutants. *B*., 293T cells were transfected with human LFA-1 and treated with different concentrations of YTA-1 mAb. *C*, SKW3 cells were pretreated with control IgG or activated with mAb CBR LFA-1/2 (10 μg/ml) or phorbol 12-myristate 13-acetate (100 μg/ml).

pretreated with YTA-1 mAb or the TS1/22 mAb to the LFA-1 α subunit I domain (Fig. 9*A*). Furthermore, the inhibition by YTA-1 was concentration-dependent (Fig. 9*B*). Similar experiments were performed using the SKW3 T lymphoma cell line. LFA-1 is endogenously expressed on these cells and binds to ICAM-1 upon stimulation with the phorbol ester phorbol 12-myristate 13-acetate or the activating mAb CBR LFA-1/2 (Fig. 9*C*). In both cases, stimulated binding was inhibited with YTA-1 and TS1/22 mAb (Fig. 9*C*).

Human but not mouse LFA-1 binds to human ICAM-1 (52), and this species specificity has been mapped to the α_L subunit I domain (29). We tested whether any of the human → mouse substitutions that affected YTA-1 binding affected binding to ICAM-1. They did not (Fig. 9*A*), demonstrating lack of involvement of these residues in species-specific recognition of LFA-1. Furthermore, this demonstrated that these substitutions did not "de-activate" LFA-1. As expected, the substitutions abolished the ability of YTA-1 mAb to block binding of LFA-1 to ICAM-1 (Fig. 9*A*).

DISCUSSION

We provide direct evidence for association between the I-like domain of integrin β subunits and the β-propeller domain of integrin α subunits. We map the epitope of the anti-LFA-1 mAb YTA-1 to specific residues in these domains, and thus localize a region of close contact between the I-like and β-propeller do-

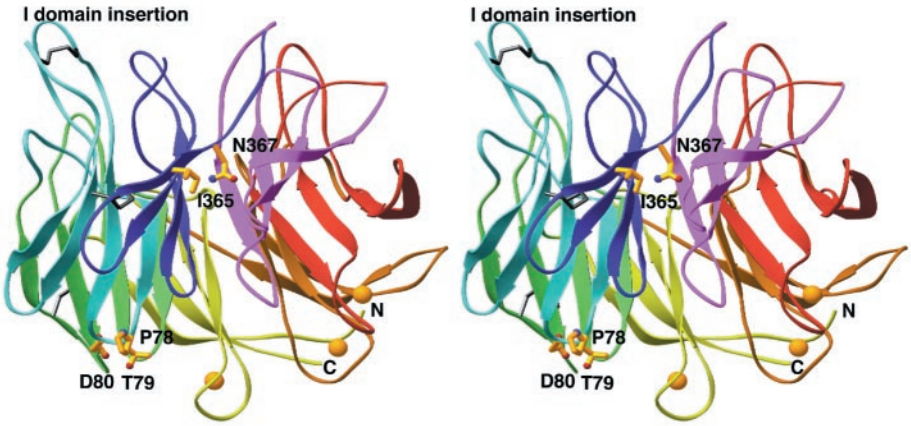

FIG. 10. **Stereodiagram of a theoretical model of the LFA-1 α subunit β-propeller domain.** Side chains for residues contributing to the YTA-1 epitope are shown in *gold*, with nitrogen and oxygen atoms shown in *blue* and *red*, respectively. Each β-sheet or W is given a different color: W1, *green*; W2, *cyan*; W3, *purple*; W4, *magenta*; W5, *red*; W6, *orange*, W7, *yellow*. The β-propeller is viewed facing W3, with its top containing the 4–1 loops up. The side containing W3 is tilted up. Three Ca^{2+} ions predicted to bind to loops on the bottom of the domain are shown as *gold spheres*. Disulfide bonds are shown in *black*. The N and C termini of the domain are at the *bottom*, and connections to the I domain at the *top*. Figure was prepared with RIBBONS (55).

mains. Interestingly, we find that YTA-1 preferentially recognizes activated LFA-1 and blocks LFA-1 binding to its ligand ICAM-1, suggesting that this specific intersubunit association is related to the active conformation of LFA-1.

Models of the LFA-1 β-propeller and I-like domains are useful for understanding our findings in three dimensions. We made an α_L subunit β-propeller model using the alignment with the transducin G protein β subunit β-propeller domain shown in Fig. 4, as described under "Materials and Methods" (Fig. 10). The approach was similar to that previously used to model α_4 and α_M β-propellers (9, 32). Residues Pro^{78}, Thr^{79}, and Asp^{80} of the YTA-1 epitope are predicted to be in a turn or loop between β-strands 1 and 2 in β-sheet 2 (W2) of the α_L subunit β-propeller (Fig. 4). Thus, they are on the lower surface of the β-propeller (Fig. 10). Residues Ile^{365} and Asn^{367} are predicted to be in β-strand 4 of W3 of the propeller (Fig. 4), located on the approximately cylindrical side of the β-propeller, about midway between the top and bottom (Fig. 10). Because β-strand 4 is the most challenging of the four β-strands in each sheet to align, the position within this β-strand should be considered tentative, whereas the alignment of β-strands 1 and 2 and hence the position of residues 78–80 in the model is straightforward. In the YTA-1 epitope, residues 365 and 367 are more important than 78–80. Introduction of the conservative substitutions V365I and Q367N into the mouse α_L subunit is sufficient to completely restore binding of YTA-1 mAb. On the other hand, the much more drastic substitutions A78P, A79T, and K80D into mouse α_L only partially reconstitute the YTA-1 epitope; therefore, it is possible that these substitutions alter the backbone structure of the loop between β strands 1 and 2, and indirectly affect the conformation of nearby residues.

Antibody competition experiments showed that mAb with epitopes localized to W1, to W2, or to W5–W7 did not block YTA-1 binding, whereas the CBR LFA-1/1 mAb localized to W3 did block YTA-1 binding. Overall, these findings localize the YTA-1 epitope on the β-propeller domain to a region centered near residues Ile^{365} and Asn^{367}, on the side of the β-propeller at blade 3.

Recently, a β_2 subunit I-like domain model was constructed that is supported by threading and secondary structure predictions, and by independent mAb epitope mapping data (57) (Fig. 11). The I-like domain was modeled using several I domains as templates. Regions of the model that are well aligned with the templates are coded with a blue ribbon backbone, and two long insertions in the I-like domain relative to the I domain, and other regions of uncertain topology, are coded with gray ribbon backbones. The previous epitope mapping studies showed that β_2 subunit residues Arg^{133} and Asn^{339} are both present in the epitope of certain mAb, and residues Arg^{133} and His^{332} are both present in another mAb's epitope. In agreement, the model predicts that these residues are on α-helices α1 and α6, which are adjacent in the structure (Fig. 11) (57). The current study identified residues Ser^{302} and Arg^{303} as the YTA-1 epitope on the β_2 subunit. Residues Ser^{302} and Arg^{303} were necessary for the YTA-1 epitope, as shown by substitution for mouse residues, and sufficient for the YTA-1 epitope, as shown by substitution into mouse β_2. Residues Ser^{302} and Arg^{303} are predicted to be in a turn between β-strand 5 and α-helix 5, at the top of the I-like domain (*gold side chains*, Fig. 11). In Fig. 11, other antigenic residues defined in β_2 are shown as *rose-pink side chains*, and the positions of antigenic residues defined in β_1 are shown as *rose-pink lollipops*. It is interesting that the antigenic residues extend only over one half of the surface of the I-like domain model (Fig. 11, *A* and *B*). In the center of this surface is the "front" face of the I-like domain, which bears helices α6, α1, and α2 (Fig. 11, *A* and *B*). All three helices bear antigenic residues, and these extend from the top to the bottom of this face. *N*-linked glycosylation sites in β integrin I-like domains are also restricted to the same half of the I-like domain surface (*gray lollipops*, Fig. 11). Residues Ser^{302} and Arg^{303}, in the β5-α5 loop, are on the top face of the I-like domain (Fig. 11*A*), and form what may be thought of as the upper-left corner of the antigenic surface (Fig. 11*B*). Glu^{175} in β_2 is on the upper right corner, in a disulfide-bonded turn (Fig. 11*B*). Viewed from the top, Ser^{302}/Arg^{303} and Glu^{175} are on opposite ends of the upper face, and in between them is the putative Mg^{2+} ion of the MIDAS of the I-like domain.

Our model and the data on the YTA-1 epitope suggest that the I-like domain associates closely at its "top left" corner in the β5-α5 loop with the β-propeller domain. It is intriguing that Ser^{302} and Arg^{303} are at the boundary between the front face, which bears antigenic and *N*-linked glycosylation sites, and the back face, which is devoid of antigenic residues and *N*-linked sites, except for one *N*-linked site near Arg^{303} on the α5 helix (Fig. 11*C*). Thus, the back face may be buried in an interface with the β-propeller domain, with Ser^{302} and Arg^{303} on the solvent exposed face near its boundary with the buried face, and hence near to the α subunit β-propeller, and to residues on its surface including Ile^{365} and Asn^{367}.

The ability of many of the mAb directed to the β subunit I-like domain to competitively inhibit binding of YTA-1 is con-

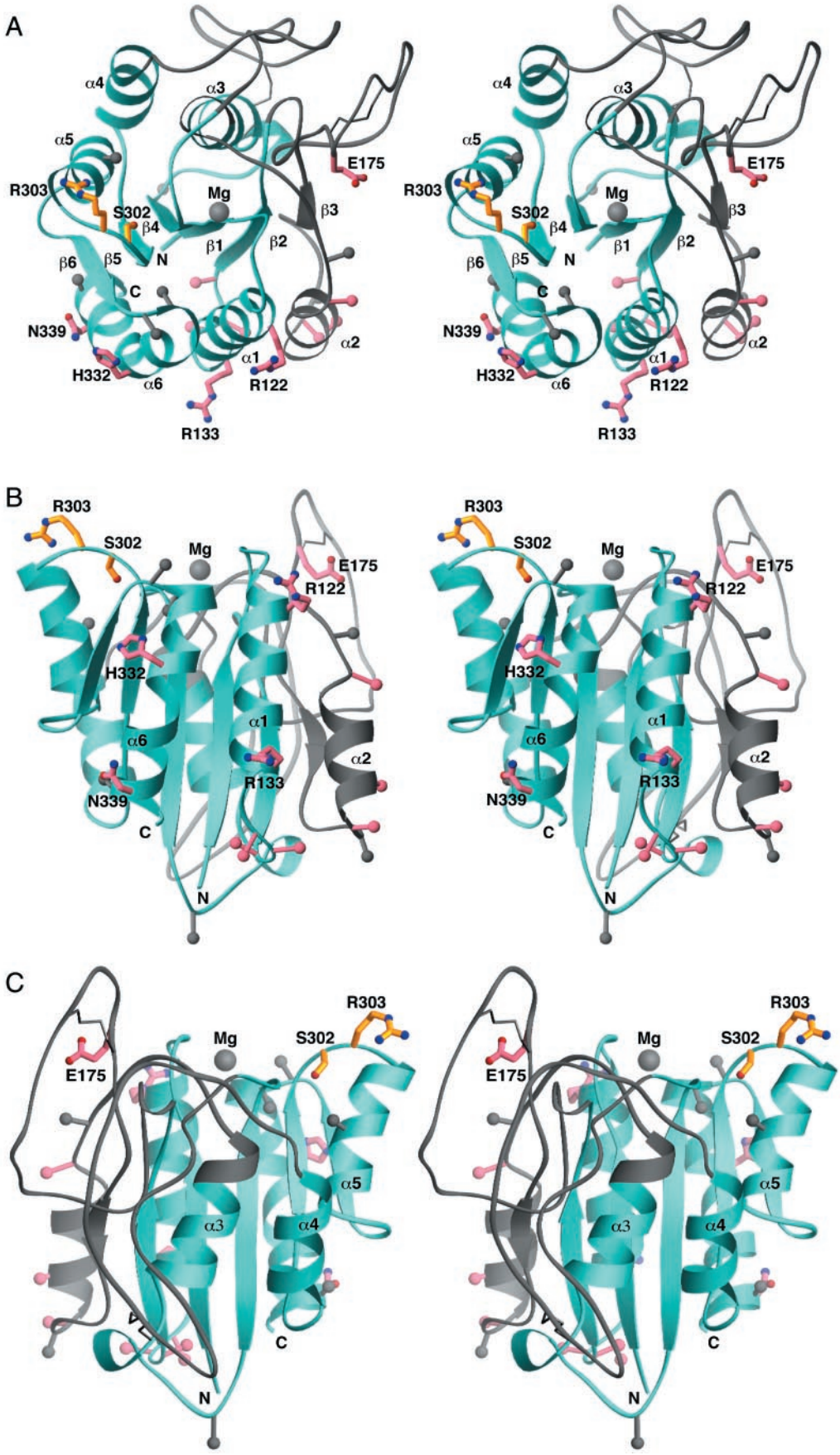

FIG. 11. **Stereodiagram of a theoretical model of the β_2 subunit I-like domain.** *A*, top view; *B*, view from the antigenic "front" face bearing the α6, α1, and α2 helices; *C*, view from the "back" face bearing the α3, α4, and α5 helices. Residues Ser^{302} and Arg^{303} in the YTA-1 epitope are shown as *gold side chains*. Other β_2 antigenic residues are shown as *rose-pink side chains* (see Footnote 2), and positions that are antigenic in β1 integrins (20, 56) are shown as *pink lollipops* with a large Cβ atom and a Cα-Cβ bond. Sites that are predicted to be *N*-glycosylated in at least 2

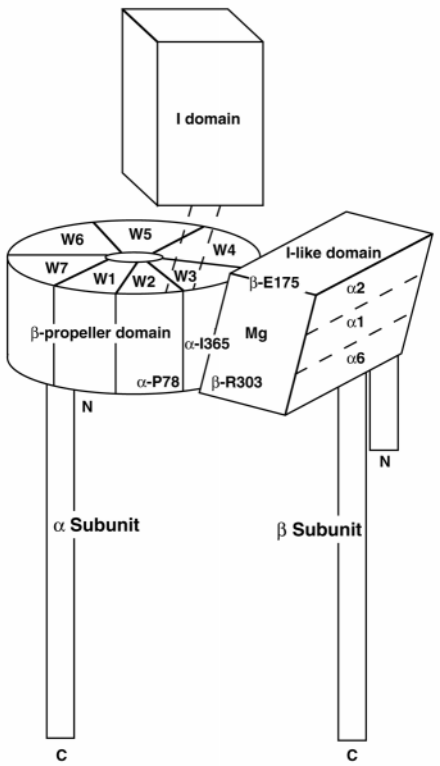

FIG. 12. **Schematic diagram of the orientation between the β-propeller and I-like domains.** The orientation is based on the points of contact defined by the YTA-1 mAb here, and the ligand mimetic mAb in (53). The top of the I-like domain contacts W3 of the β-propeller, with the edge bearing β-Ser^{302} and β-Arg^{303} and β-strand 6 of the I-like domain near the lower half of W2 and W3 of the β-propeller, bearing α-Pro^{78}, α-Thr^{79}, α-Asp^{80}, α-Ile^{365}, and α-Asn^{367}, as shown with the YTA-1 mAb; and the edge bearing the specificity-determining loop with β-Glu^{175} and β-strand 3 near the top of W3, as shown with ligand-mimetic mAb to $\alpha_{IIb}\beta_3$.

sistent with the proximity of the antigenic residues to one another on the same side of the I-like domain (Fig. 11, *A* and *B*). In the model, Cα distances are 18 Å between Ser^{302} and His^{322}, and 22 Å between Ser^{302} and Glu^{175}. Since antibodies have footprints about 30 Å in diameter, there could easily be overlap between the footprints of YTA-1 recognizing Ser^{302} and other antibodies recognizing His^{322} or Glu^{175}, giving competition between antibody binding. However, there also could be an indirect interaction between the YTA-1 epitope and residues Arg^{133} and His^{332}. Knockout of both Arg^{133} and His^{332}, but not either residue alone, abolished binding of YTA-1. In contrast, knock-in of both of these residues yielded no reconstitution of the YTA-1 epitope whatsoever. Furthermore, some mAb that bind to Arg^{133} and His^{332} did not block binding of YTA-1, and blocking was variable depending on the cell type examined. Indirect effects on the YTA-1 epitope may occur because this epitope is dependent on the activation state of LFA-1. Therefore, we have been careful throughout this study to use two independent methods to identify residues directly involved in the YTA-1 epitope: human to mouse mutations to decrease or abolish YTA-1 binding, and mouse to human mutations to reconstitute YTA-1 binding.

The YTA-1 epitope mapping results lead us to the conclusion that the top edge of the I-like domain associates with the side of the β-propeller domain at β-sheets 2 and 3. These data establish a point of contact between these domains, but not their orientation relative to one another. Interestingly, a second point of contact has very recently been revealed between the α_{IIb} β-propeller domain and the β_3 I-like domain in elegant work by Takada and co-workers (53) that mapped ligand-mimetic antibodies. The residues recognized by these mAb in β_3 are present in the same disulfide-bonded loop that contains Glu^{175} in β_2; thus, this contact region is on the top face of the I-like domain on the edge opposite from Ser^{302} and Arg^{303} (Fig. 11, *A* and *B*). This same loop has been demonstrated to bear specificity for ligand and has been termed the specificity-determining loop (53, 54). The contact residues in α_{IIb} are in the 4–1 loops at the top edge of the β-propeller, between β-sheets 2 and 3, and between β-sheets 3 and 4. Thus, both YTA-1 to LFA-1 and the ligand mimetic antibodies to $\alpha_{IIb}\beta_3$ contact the β-propeller on the side with β-sheet 3, but the ligand-mimetic-defined contact is at the top of the side, whereas the YTA-1-defined contact is on the middle to bottom of the side. With two points of contact, the relative orientation of the β-propeller and I-like domains can be predicted (Fig. 12). The top of the I-like domain is in contact with the side of the β-propeller domain. Furthermore, the edge of the I-like domain with β-strand 3 and α-helix 2 is toward the top of the β-propeller, whereas the edge with β-strand 6 and α-helix 6 is toward the bottom of the β-propeller. It is tempting to speculate that the back face of the I-like domain, which lacks antigenic residues and *N*-linked sites, is in contact with the β-propeller. If so, then the orientation defined by the epitopes would mean that with the top of I-like domain contacting the β-propeller near β-sheet 3, the bottom would extend toward β-sheet 5, rather than toward β-sheet 1 (Fig. 12). Note that the putative MIDAS motif is positioned in the middle of the interface between the β-propeller and I-like domain, as appropriate for a function in ligand binding, or in regulating the conformation of loops involved in ligand binding. The I-like domain MIDAS and the specificity-determining loop are well situated to interact with ligand-binding loops on the upper surface of the β-propeller in β-sheets 2, 3, and 4 of the α_{IIb}, α_4, and α_5 integrins (see Introduction for references).

The I domain is inserted into a loop at the top of the β-propeller domain, between β-sheets 2 and 3. Therefore, the bottom of the I domain is in close proximity to the top of the I-like domain. The C-terminal α-helix of the I domain moves 10 Å down the side of the domain in a movement that is linked to a shift from a putative inactive to active ligand binding configuration at the top of the domain (31). Therefore, the interface between the α subunit β-propeller and β subunit I-like domains is well positioned both to indirectly regulate ligand binding by I domain-containing integrins, and directly participate in ligand binding by integrins that lack I domains. We have shown here that the YTA-1 mAb selectively binds to activated LFA-1. Thus, the interface it recognizes between the β-propeller domain and I-like domain appears to alter structurally during activation of LFA-1, and may be an important linkage in the machinery for inside-out signal transduction by integrins.

Acknowledgments—We thank Dr. Katsuji Sugie and Dr. Junji Yodoi for kindly providing the mAb YTA-1, Mark Ryan for technical assistance on fluorescence-activated cell sorting analysis, and Dr. Paddy Yalamanchili for critical review of this manuscript.

REFERENCES

1. Springer, T. A. (1990) *Nature* **346,** 425–433
2. Van der Vieren, M., Le Trong, H., Wood, C. L., Moore, P. F., St. John, T.,

of 35 integrin β subunits are shown as *gray lollipops*. See Footnote 2 for preparation of the model. The ribbon trace for regions of the model that are well aligned to the I-domain templates is *blue* and for regions of insertions or uncertain topology is *gray*. The hypothetical Mg^{2+} bound to the MIDAS is shown as a gray sphere. Fog is used as a depth cue. Figure was prepared with RIBBONS (55).

Staunton, D. E., and Gallatin, W. M. (1995) *Immunity* **3,** 683–690
3. Kishimoto, T. K., O'Connor, K., Lee, A., Roberts, T. M., and Springer, T. A. (1987) *Cell* **48,** 681–690
4. Marlin, S. D., and Springer, T. A. (1987) *Cell* **51,** 813–819
5. Staunton, D. E., Dustin, M. L., and Springer, T. A. (1989) *Nature* **339,** 61–64
6. de Fougerolles, A. R., Stacker, S. A., Schwarting, R., and Springer, T. A. (1991) *J. Exp. Med.* **174,** 253–267
7. Springer, T. A., Dustin, M. L., Kishimoto, T. K., and Marlin, S. D. (1987) *Annu. Rev. Immunol.* **5,** 223–252
8. Larson, R. S., and Springer, T. A. (1990) *Immunol. Rev.* **114,** 181–217
9. Springer, T. A. (1997) *Proc. Natl. Acad. Sci. U. S. A.* **94,** 65–72
10. Kamata, T., Puzon, W., and Takada, Y. (1995) *Biochem. J.* **305,** 945–951
11. Schiffer, S. G., Hemler, M. E., Lobb, R. R., Tizard, R., and Osborn, L. (1995) *J. Biol. Chem.* **270,** 14270–14273
12. Irie, A., Kamata, T., Puzon-McLaughlin, W., and Takada, Y. (1995) *EMBO J.* **14,** 5550–5556
13. Mould, A. P., Askari, J. A., Aota, S., Yamada, K. M., Irie, A., Takada, Y., Mardon, H. J., and Humphries, M. J. (1997) *J. Biol. Chem.* **272,** 17283–17292
14. Kamata, T., Irie, A., Tokuhira, M., and Takada, Y. (1996) *J. Biol. Chem.* **271,** 18610–18615
15. Lee, J.-O., Rieu, P., Arnaout, M. A., and Liddington, R. (1995) *Cell* **80,** 631–638
16. Qu, A., and Leahy, D. J. (1995) *Proc. Natl. Acad. Sci. U. S. A.* **92,** 10277–10281
17. Tozer, E. C., Liddington, R. C., Sutcliffe, M. J., Smeeton, A. H., and Loftus, J. C. (1996) *J. Biol. Chem.* **271,** 21978–21984
18. Tuckwell, D. S., and Humphries, M. J. (1997) *FEBS Lett.* **400,** 297–303
19. Puzon-McLaughlin, W., and Takada, Y. (1996) *J. Biol. Chem.* **271,** 20438–20443
20. Shih, D. T., Doettiger, D., and Buck, C. A. (1997) *J. Cell Sci.* **110,** 2619–2628
21. Dransfield, I., and Hogg, N. (1989) *EMBO J.* **8,** 3759–3765
22. Dransfield, I., Cabañas, C., Craig, A., and Hogg, N. (1992) *J. Cell Biol.* **116,** 219–226
23. Loftus, J. C., O'Toole, T. E., Plow, E. F., Glass, A., Frelinger, A. L., III, and Ginsberg, M. H. (1990) *Science* **249,** 915–918
24. Gailit, J., and Ruoslahti, E. (1988) *J. Biol. Chem.* **263,** 12927–12932
25. van Kooyk, Y., Weder, P., Heije, K., and Figdor, C. G. (1994) *J. Cell Biol.* **124,** 1061–1070
26. Randi, A. M., and Hogg, N. (1994) *J. Biol. Chem.* **269,** 12395–12398
27. Edwards, C. P., Champe, M., Gonzalez, T., Wessinger, M. E., Spencer, S. A., Presta, L. G., Berman, P. W., and Bodary, S. C. (1995) *J. Biol. Chem.* **270,** 12635–12640
28. Bajt, M. L., Goodman, T., and McGuire, S. L. (1995) *J. Biol. Chem.* **270,** 94–98
29. Huang, C., and Springer, T. A. (1995) *J. Biol. Chem.* **270,** 19008–19016
30. van Kooyk, Y., Binnerts, M. E., Edwards, C. P., Champe, M., Berman, P. W., Figdor, C. G., and Bodary, S. C. (1996) *J. Exp. Med.* **183,** 1247–1252
31. Lee, J.-O., Bankston, L. A., Arnaout, M. A., and Liddington, R. C. (1995) *Structure* **3,** 1333–1340
32. Oxvig, C., Lu, C., and Springer, T. A. (1999) *Proc. Natl. Acad. Sci. U. S. A.* **96,** 2215–2220
33. McDowall, A., Leitinger, B., Stanley, P., Bates, P. A., Randi, A. M., and Hogg, N. (1998) *J. Biol. Chem.* **273,** 27396–27403
34. Li, R., Rieu, P., Griffith, D. L., Scott, D., and Arnaout, M. A. (1998) *J. Cell Biol.* **143,** 1523–1534
35. Huang, C., Lu, C., and Springer, T. A. (1997) *Proc. Natl. Acad. Sci. U. S. A.* **94,** 3156–3161
36. Huang, C., and Springer, T. A. (1997) *Proc. Natl. Acad. Sci. U. S. A.* **94,** 3162–3167
37. Sugie, K., Nakamura, K., Teshigawara, K., Diamond, M. S., Springer, T. A., Nakamura, Y., Leonard, W. J., Uchida, A., and Yodoi, J. (1995) *Int. Immunol.* **7,** 763–769
38. Sugie, K., Minami, Y., Kawakami, T., and Uchida, A. (1995) *Int. Immunol.* **154,** 1691–1698
39. Sanchez-Madrid, F., Krensky, A. M., Ware, C. F., Robbins, E., Strominger, J. L., Burakoff, S. J., and Springer, T. A. (1982) *Proc. Natl. Acad. Sci. U. S. A.* **79,** 7489–7493
40. Sanchez-Madrid, F., Davignon, D., Martz, E., and Springer, T. A. (1982) *Cell Immunol.* **73,** 1–11
41. Ho, S. N., Hunt, H. D., Horton, R. M., Pullen, J. K., and Pease, L. R. (1989) *Gene* (*Amst.*) **77,** 51–59
42. Heinzel, S. S., Krysan, P. J., Calos, M. P., and DuBridge, R. B. (1988) *J. Virol.* **62,** 3738–3746
43. DuBridge, R. B., Tang, P., Hsia, H. C., Leong, P. M., Miller, J. H., and Calos, M. P. (1987) *Mol. Cell. Biol.* **7,** 379–387
44. Lu, C., and Springer, T. A. (1997) *J. Immunol.* **159,** 268–278
45. Levitt, M. (1992) *J. Mol. Biol.* **226,** 507–533
46. Sali, A., and Blundell, T. L. (1993) *J. Mol. Biol.* **234,** 779–815
47. Sondek, J., Bohm, A., Lambright, D. G., Hamm, H. E., and Sigler, P. B. (1996) *Nature* **379,** 369–374
48. Oxvig, C., and Springer, T. A. (1998) *Proc. Natl. Acad. Sci. U. S. A.* **95,** 4870–4875
49. Vriend, G. (1990) *J. Mol. Graph.* **8,** 52–56
50. Hibbs, M. L., Wardlaw, A. J., Stacker, S. A., Anderson, D. C., Lee, A., Roberts, T. M., and Springer, T. A. (1990) *J. Clin. Invest.* **85,** 674–681
51. Larson, R. S., Hibbs, M. L., and Springer, T. A. (1990) *Cell Regul.* **1,** 359–367
52. Johnston, S. C., Dustin, M. L., Hibbs, M. L., and Springer, T. A. (1990) *J. Immunol.* **145,** 1181–1187
53. Puzon-McLaughlin, W., Kamata, T., and Takada, Y. (2000) *J. Biol. Chem.* **275,** 7795–7802
54. Takagi, J., Kamata, T., Meredith, J., Puzon-McLaughlin, W., and Takada, Y. (1997) *J. Biol. Chem.* **272,** 19794–19800
55. Carson, M. (1997) *Methods Enzymol.* **277,** 493–505
56. Takada, Y., and Puzon, W. (1993) *J. Biol. Chem.* **268,** 17597–17601
57. Huang, C., Zang, Q., Takagi, J., and Springer, T. A. (2000) *J. Biol. Chem.* **275,** 21514–21524